square of input phase and amplitude, but is still much simpler than using the actual formulas. The approximation has shown to predict well the penalty due to GVD in a singlemode fiber.

References

[1] A. R. Chraplyvy, R. W. Tkach, L. L. Buhl, and R. C. Alferness, "Phase modulation to amplitude conversion of CW laser light in optical fibers," *Electron. Lett.*, vol. 22, pp. 409–411, Feb. 1986.

[2] K. Tajima, "Self amplitude modulation in PSK coherent optical transmission systems," *J. Lightwave Technol.*, vol. 4, no. 7, pp. 900–904, July 1986.

[3] A. F. Elrefaie, R. E. Wagner, D. A. Atlas, and D. G. Daut, "Chromatic dispersion limitations in coherent lightwave transmission systems," *J. Lightwave Technol.*, vol. 6, no. 5, pp. 704–709, May 1988.

[4] J. Wang and K. Petermann, "Small signal analysis for dispersive optical fiber communications systems, " *J. Lightwave Technol.*, vol. 10, no. 1, pp. 96–100, Jan. 1992.

[5] C Crognale, "Small signal frequency response of a linear dispersive single-mode fiber near zero first-order dispersion wavelength," *J. Lightwave Technol.*, vol. 15, no. 3, pp. 482–489, March 1997.

[6] E. Bedrosian and S. O. Rice, "Distorsion and crosstalk of linearly filtered, angle-modulated signals," *Proc. IEEE*, vol. 56, no. 5, pp. 2–13, Jan. 1968.

[7] R. G. Mckay and J. C. Cartledge, "Performance of coherent optical CPFSK-DD with intersymbol interference, noise correlation, and laser phase noise," *J. Lightwave Technol.*, vol. 11, no. 11, pp. 1845–1853, Nov. 1993.

[8] E. Forestieri, G. Prati, "Theoretical analysis of coherent optical FSK systems with limiter-discriminator detection," *IEEE Trans. on Communications*, vol. 42, pp. 562–573, Feb. 1994.

[9] E. Forestieri, G. Prati, " Analysis of delay-and-multiply optical FSK receivers with line coding and non-flat laser FM response," *IEEE J. Select. Areas Commun.*, vol 13, pp. 543–556, Apr. 1995.

SPM/XPM-Induced Intensity Distortion in WDM systems

A. Bononi, G. Bellotti, M. Varani, and C. Francia

Dipartimento di Ingegneria dell'Informazione, Università di Parma, Viale delle Scienze I-43100 Parma, Italy

Abstract: In high bit-rate multiwavelength optical transmission systems, self-phase (SPM) and cross-phase (XPM) modulation interact with the fiber chromatic dispersion producing intensity distortion on the transmitted signals.
In this paper, starting from a generalization of the model of Wang and Petermann [1], which approximately predicts the effect of phase-to-intensity modulation (PM/IM) conversion in purely linear fibers, we introduce a new analytical model of the intensity distortions induced by SPM and XPM. The model well captures the distributed generation of SPM (XPM) by accounting for the PM/IM conversion due to the infinitesimal SPM (XPM) components generated in each infinitesimal segment along the fiber.

1. Introduction

At the large transmission powers needed in high bit-rate multi-span wavelength division multiplexed (WDM) communication systems with in-line fiber amplifiers and dispersion management, the interplay between nonlinear phase modulation, i.e., self-phase (SPM) and cross-phase modulation (XPM), and group-velocity dispersion (GVD) plays a primary role in setting the limits to system performance [2], [3].

An accurate study of such interactions must necessarily resort to a time consuming numerical solution of the nonlinear Schrödinger equation (NLSE), since a general analytical solution for non-soliton input pulses is not available when both the dispersive and the nonlinear terms are present [4].

Thus, simple approximate analytical models that capture the essence of this interplay have been proposed, by either introducing approximations in the NLSE or resorting to phenomenological approaches, both in single-channel systems [5], and in multichannel systems [6], [7], [8], [9], [10].

In [6]–[9] a linear model for the interaction between XPM and GVD was proposed, based on a model for phase-to-intensity modulation (PM/IM) conversion in linear fibers [1]. It works as follows. A high-power modulated pump signal induces XPM on a weak probe continuous wave (CW) signal. The XPM on the probe at the end of the link is the sum of the XPM contributions generated in each infinitesimal fiber segment. Each infinitesimal XPM contribution gives an infinitesimal intensity distortion (or noise, if the XPM is considered as a random process) by PM/IM conversion at the end of the link. Such infinitesimal contributions *add up* to give the total output probe intensity distortion. The main assumptions in the model are:

1) the probe is low-power, which allows to neglect the interaction between XPM and the SPM on the probe;

2) the probe channel is CW, which allows to define an average intensity level to which the relative intensity noise (RIN) is referred;

3) the RIN is small with respect to the average intensity at all points along the link, which is the basic assumption of the linear model in [1];

4) The modulated pump intensity is only attenuated but not distorted during propagation.

In this paper we mitigate assumption 4) by assuming the pump is distorted by GVD only. Comparisons with accurate numerical solutions of the NLSE show that this model is valid over a broad range of system parameters, which encompass all practical terrestrial WDM dispersion managed systems at bit rates per channel up to 40 Gb/s.

Following the same idea, but starting from a generalization of the theory in [1], we also present a model for the interaction between SPM and GVD. This SPM/AM model, whose accuracy is inferior to the XPM/IM one, can nonetheless be of significant value in the understanding of the SPM/GVD interplay.

2. Generalization of the Wang-Petermann Model

Consider the propagation along a linear, single-mode, lossless fiber of length L. The fiber operates on the complex envelope $E_{in}(t)$ (relative to a reference frequency $\Omega = 2\pi c/\lambda$, c being the speed of light and λ the reference wavelength) of the input electric field with a lowpass equivalent filter with frequency response given by [11]:

$$H(\omega) = e^{-j\Upsilon L\omega^2 - j\Gamma L\omega^3} \tag{1}$$

where

$$\Upsilon \triangleq -\frac{\lambda^2 D}{4\pi c}, \qquad \Gamma \triangleq \frac{\lambda^2}{6(2\pi c)^2}\left(2\lambda D + \lambda^2 \frac{\partial D}{\partial \lambda}\right)$$

ω is the frequency offset from Ω, and D and $\frac{\partial D}{\partial \lambda}$ are the fiber dispersion parameter and dispersion slope, respectively, at the reference wavelength λ. In (1) only the first- and second-order chromatic dispersion terms have been taken into account. First-order dispersion is known as group-velocity dispersion (GVD). The inverse transform of (1), when only GVD is accounted for, is:

$$h(t) = \begin{cases} \dfrac{e^{j\frac{t^2}{4\Upsilon L}}}{\sqrt{8\pi\Upsilon L}}(1-j) & \text{for } \Upsilon > 0 \\ \dfrac{e^{j\frac{t^2}{4\Upsilon L}}}{\sqrt{8\pi|\Upsilon|L}}(1+j) & \text{for } \Upsilon < 0 \end{cases} \tag{2}$$

It is useful for later purposes to write the impulse response in its real and imaginary components: $h(t) = h_R(t) + jh_I(t)$, which are obtained from (2) as:

$$\begin{cases} h_R(t) = \dfrac{1}{\sqrt{8\pi|\Upsilon|L}}\left[\sin\left(\dfrac{t^2}{4|\Upsilon|L}\right) + \cos\left(\dfrac{t^2}{4|\Upsilon|L}\right)\right] \\ h_I(t) = \dfrac{\operatorname{sgn}(\Upsilon)}{\sqrt{8\pi|\Upsilon|L}}\left[\sin\left(\dfrac{t^2}{4|\Upsilon|L}\right) - \cos\left(\dfrac{t^2}{4|\Upsilon|L}\right)\right] \end{cases} \tag{3}$$

Similarly, in the frequency domain the equivalent lowpass fiber frequency response ((1), with $\Gamma = 0$) can be written as the sum of its real and imaginary part $H(\omega) = H_R(\omega) + jH_I(\omega)$:

$$\begin{cases} H_R(\omega) = \cos(\Upsilon L\omega^2) \\ H_I(\omega) = -\sin(\Upsilon L\omega^2) \end{cases} \tag{4}$$

and since both $H_R(\omega)$ and $H_I(\omega)$ are real and even, their inverse transforms are real and coincide with the real and imaginary components of the impulse response $h_R(t)$ and $h_I(t)$.

The complex envelope of the output field is obtained as the convolution ($\otimes$) of the input envelope and the impulse response:

$$E_{out}(t) = E_{in}(t) \otimes h(t) \tag{5}$$

The output field has intensity[1] $P_{out}(t) \triangleq |E_{out}(t)|^2$ and therefore the relation between the input and output initensities is not linear.

In a well-known paper [1], Wang and Petermann gave a small signal linear relation between the input and output phases and intensities, in the assumption of a fiber with only GVD ($\Gamma = 0$ in (1)). Here we provide a generalization of such model.

Let $E_{in}(t) \triangleq a_{in}(t)e^{j\theta_{in}(t)}$ be the fiber input field, where a_{in} and θ_{in} are real quantities representing the field magnitude and the field phase, respectively. Define similarly the output field as $E_{out}(t) \triangleq a_{out}(t)e^{j\theta_{out}(t)}$. The input and output intensities are thus $P_{in}(t) = a_{in}^2(t)$ and $P_{out}(t) = a_{out}^2(t)$, respectively.

From (5) we get:

$$a_{out}(t)e^{j\theta_{out}(t)} = \left[a_{in}(t)e^{j\theta_{in}(t)}\right] \otimes [h_R(t) + jh_I(t)] \tag{6}$$

We now want to get linear relations between the field input and output phase and magnitude. To this goal, we define $a_{in}(t) \triangleq <A_{in}> + \Delta a_{in}(t)$ and $a_{out}(t) \triangleq <A_{out}> + \Delta a_{out}(t)$, where we introduced an arbitrary average input magnitude $<A_{in}>$ and output magnitude $<A_{out}>$, and defined the perturbations $\Delta a_{in}(t)$ and $\Delta a_{out}(t)$ of such averages. In the hypothesis of small

[1] We use normalized complex fields whose units are $\sqrt{W}$, so that the intensity is measured in W.

amplitude perturbation ($|\Delta a_{in}(t)| \ll <A_{in}>$ and $|\Delta a_{out}(t)| \ll <A_{out}>$), we can expand the exponential $e^x \simeq 1+x$ and eq. (6) becomes:

$$\begin{aligned}&<A_{out}> + \Delta a_{out}(t) + j <A_{out}> \theta_{out}(t) = \\ &[<A_{out}> + \Delta a_{out}(t) + j <A_{out}> \theta_{out}(t)] \otimes [h_R(t) + j h_I(t)]\end{aligned} \tag{7}$$

Using $h_R(t) \otimes 1 = 1$, and $h_I(t) \otimes 1 = 0$, and assuming without loss of generality $<A_{in}>=<A_{out}>=<A>$, we get:

$$\begin{cases} \Delta a_{out}(t) \simeq -<A> (h_I(t) \otimes \theta_{in}(t)) + h_R(t) \otimes \Delta a_{in}(t) \\ \theta_{out}(t) \quad \simeq h_R(t) \otimes \theta_{in}(t) + h_I(t) \otimes \frac{\Delta a_{in}(t)}{<A>} \end{cases} \tag{8}$$

or equivalently:

$$\begin{cases} a_{out}(t) \simeq -<A> (h_I(t) \otimes \theta_{in}(t)) + h_R(t) \otimes a_{in}(t) \\ \theta_{out}(t) \simeq h_R(t) \otimes \theta_{in}(t) + h_I(t) \otimes \frac{a_{in}(t)}{<A>} \end{cases} \tag{9}$$

Relations (8) and (9) represent the sought generalizations of the Wang–Petermann formulae ([1], eq. (27)), but applied to the electric field instead of its intensity. They also apply not only to the fiber, in which chromatic dispersion is expanded to any order, but also to general optical filters $h(t)$. Transforming (8) and using the fiber frequency response components (4) we get:

$$\begin{pmatrix} \frac{\Delta a_{out}(\omega)}{<A>} \\ \theta_{out}(\omega) \end{pmatrix} = \begin{pmatrix} \cos(\Upsilon L\omega^2) & \sin(\Upsilon L\omega^2) \\ -\sin(\Upsilon L\omega^2) & \cos(\Upsilon L\omega^2) \end{pmatrix} \begin{pmatrix} \frac{\Delta A_{in}(\omega)}{<A>} \\ \theta_{in}(\omega) \end{pmatrix} \tag{10}$$

Note that, for $\theta_{in}(t) = 0$, eq. (9) reduces to $a_{out}(t) \simeq h_R(t) \otimes a_{in}(t)$. In the frequency domain: $A_{out}(\omega) \simeq H_R(\omega) A_{in}(\omega)$. Observing that the exact expression is $A_{out}(\omega) \simeq [H_R(\omega) + jH_I(\omega)]A_{in}(\omega)$, the small amplitude approximation corresponds to neglecting $H_I(\omega)$ with respect to $H_R(\omega)$. Such approximation is valid when $\tan \frac{\lambda^2 \omega^2 DL}{4\pi c} \ll 1$, that is:

$$\omega^2 \ll \frac{\pi c}{\lambda^2 DL} \tag{11}$$

This means that the approximation is more accurate when the the signal spectrum is narrow and the accumulated dispersion DL is low.

The Wang–Petermann formulae ([1], eq. (27)) can be simply obtained by making the further approximations: $P_{in}(t) \triangleq <P> (1 + \frac{\Delta P_{in}(\omega)}{<P>}) \simeq <A>^2 (1 + \frac{2\Delta A_{in}(\omega)}{<A>})$ and $P_{out}(t) \triangleq <P> (1 + \frac{\Delta P_{out}(\omega)}{<P>}) \simeq <A>^2 (1 + \frac{2\Delta A_{out}(\omega)}{<A>})$, where $<P>$ is the time-averaged intensity, and $\Delta P_{in}(t)$, $\Delta P_{out}(t)$ the small intensity perturbation terms. As an example, in Fig. 1 the predictions of the output intensities obtained with the Wang–Petermann formulae (left, dashed line) and the generalized one (right, dashed line) are compared, for a system composed of a single span of 50 km standard single-mode fiber (SMF, D=17 ps/km/nm). The output intensity obtained by simulation is represented by a thick line, while the thin line represents the input intensity. The better prediction of the generalized model is evident.

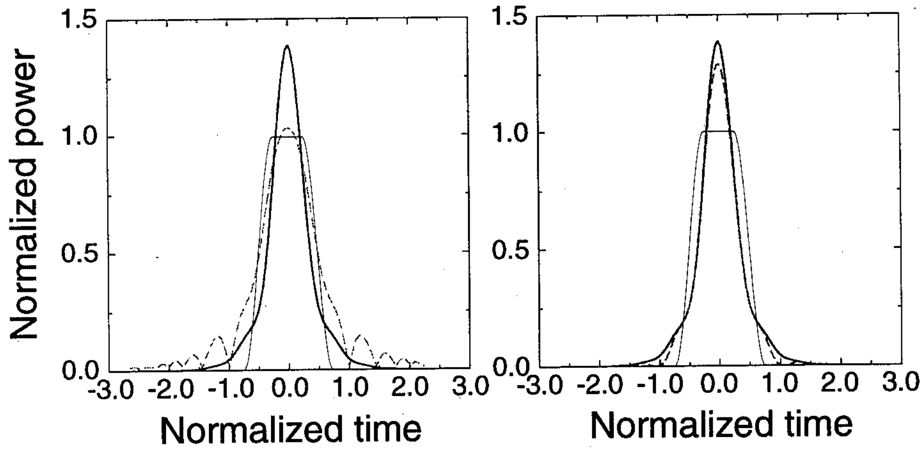

Fig. 1. Comparison between Wang–Petermann model and generalized model.

3. Intensity Distortion Induced by XPM

XPM is a simple phase modulation which has the only particularity that grows in a distributed way during the propagation along the fiber. After its generation, like every phase modulation, XPM is converted to intensity noise by means of the PM/IM conversion induced by GVD. Analytically, we can take into account this distributed generation by supposing that the overall intensity noise is the sum of the contributions of XPM generated in each infinitesimal fiber segment, each one converted to intensity modulation by the dispersion accumulated from this segment to the end of the fiber link.

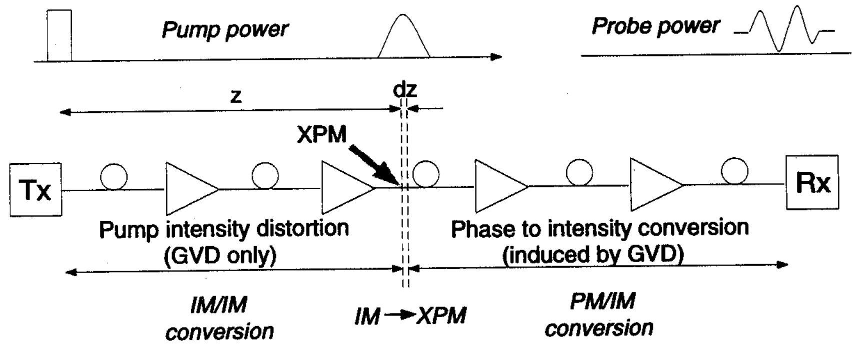

Fig. 2. Graphical interpretation of the theoretical model for the XPM-induced intensity distortion.

The key idea for our model is presented in Fig. 2. We consider an initially monochromatic probe channel and an intensity modulated pump channel. In each infinitesimal segment dz of the multi-span fiber link, the intensity modulation of the pump induces, through XPM, a phase modulation on the probe. This infinitesimal phase modulation of the probe is then converted to amplitude modulation through PM/AM conversion by the overall dispersion accumulated from the distance z to the receiver. The conversion can be calculated using the generalized Wang–Petermann model. At the receiver, the overall intensity distortion on the probe is simply the sum, that is the integral, of the contributions of intensity distortion generated in each infinitesimal segment dz of the fiber. The problem is the knowledge of the pump power at the distance z. Here, the shape of the pump is distorted because of the GVD, SPM and XPM accumulated during the propagation from the transmitter to the distance z. In a previous model [8], [9], we supposed that the pump intensity distortion was indistorted during the propagation. This assumption has been made also for two models very similar to our [6], [7]. Here, we improve the model, by removing this assumption, and supposing that the pump power is distorted only by GVD, which, during the propagation, is the major cause of intensity distortion, in particular at high bit rate. In fact, this less stringent hypotesis allows the model to be valid for bit rates up to 40 Gb/s.

Consider one span of single-mode fiber of length L, with two co-propagating channels, s and p, having the same polarization. *Probe* channel s is continuous-wave (CW), while *pump* channel p is intensity modulated, being $P_p(0,\omega)$ the Fourier transform of its power at the beginning of the fiber. Let v_s and v_p be the group velocities of the two channels, and let $d_{sp} \triangleq 1/v_s - 1/v_p \cong D\,\Delta\lambda_{sp}$ be the walk-off parameter [12], with D the fiber dispersion at the probe wavelength and $\Delta\lambda_{sp}$ the channel spacing.

The pump power at coordinate z along the fiber, in the assumption that the interfering channel intensity distortion is due to GVD only, has Fourier transform (with respect to a time frame moving with the probe group velocity) given by:

$$P_p(z,\omega) \triangleq P_p(0,\omega)e^{(-\alpha+j\omega d_{sp})z}\cos\left[\omega^2\frac{\lambda^2}{4\pi c}Dz\right] \tag{12}$$

The imaginary argument of the exponential term accounts for the time shift due to channel walk-off, while the cosine term accounts for the intensity-to-intensity conversion induced by GVD in the assumption of small perturbations [1].

The probe phase induced at z through XPM by propagation of such pump over an infinitesimal segment dz is:

$$d\theta_{sp}(z,\omega) = -2\gamma P_p(z,\omega)dz \tag{13}$$

Such phase modulation enters the remaining $L-z$ km of fiber: if such fiber were purely linear, it would produce at its output a relative probe amplitude distortion (see eq. (10)):

$$\frac{dA_{sp}(z,\omega)}{<A_s>} = -\sin\left[\omega^2\frac{\lambda^2}{4\pi c}D(L-z)\right]d\theta_{sp}(z,\omega) \tag{14}$$

where $<P_s>$ is the time averaged output probe power, λ the probe wavelength and c the light velocity.

The total relative output amplitude distortion on the probe is obtained by integrating (14) in dz over the fiber length:

$$\frac{\Delta A_{sp}(\omega)}{<A_s>} = P_p(0,\omega)H_{sp}(\omega) \tag{15}$$

where we defined the XPM/AM filter as:

$$\begin{aligned}H_{sp}(\omega) &\triangleq 2\gamma\int_0^L\left\{e^{(-\alpha+j\omega d_{sp})z}\cos\left[\omega^2\frac{\lambda^2}{4\pi c}Dz\right]\cdot\sin\left[\omega^2\frac{\lambda^2}{4\pi c}D(L-z)\right]\right\}dz\\ &= 2\gamma\left\{\frac{1}{4j}e^{j\omega^2\frac{\lambda^2}{4\pi c}[D_r-D_a]}\frac{1-e^{\left(-\alpha+j\omega d_{sp}-2jD\omega^2\frac{\lambda^2}{4\pi c}\right)L}}{\alpha-j\omega d_{sp}+2jD\omega^2\frac{\lambda^2}{4\pi c}}\right.\\ &\quad-\frac{1}{4j}e^{-j\omega^2\frac{\lambda^2}{4\pi c}[D_r-D_a]}\frac{1-e^{\left(-\alpha+j\omega d_{sp}+2jD\omega^2\frac{\lambda^2}{4\pi c}\right)L}}{\alpha-j\omega d_{sp}-2jD\omega^2\frac{\lambda^2}{4\pi c}}\\ &\quad\left.+\frac{1}{2}\sin\left[\frac{\lambda^2}{4\pi c}\omega^2(D_r+D_a)\right]\frac{1-e^{(-\alpha+j\omega d_{sp})L}}{\alpha-j\omega d_{sp}}\right\}\end{aligned} \tag{16}$$

where D_r is the residual dispersion accumulated from the beginning of the fiber to the end of the system, here $D_r = DL$, and D_a is the dispersion accumulated from the beginning of the system to the beginning of the fiber, here $D_a = 0$.

Consider now the general case of a chain of M end-amplified fiber links, with $\alpha_i, \gamma_i, D_i, l_i, d_{sp}^{(i)}$ the attenuation, nonlinear and dispersion coefficients, the length and the walk-off parameter of the i-th link, $i = 1, \ldots, M$, respectively. Suppose that the i-th amplifier has gain $G_p^{(i)}$ for the pump, so that the pump power at coordinate z of the k-th link, in our assumptions, is

$$P_p(L_k+z,\omega) = C_p^{(k)}P_p(0,\omega)e^{(-\alpha_k+j\omega d_{sp}^{(k)})z}\cos\left[\omega^2\frac{\lambda^2}{4\pi c}(D_a^{(k)}+D_kz)\right] \tag{17}$$

where $L_k \triangleq \sum_{i=1}^{k-1} l_i$, $C_p^{(k)} \triangleq \prod_{i=1}^{k-1} e^{(-\alpha_i+j\omega d_{sp}^{(i)})l_i}G_p^{(i)}$, $C_p^{(1)} \triangleq 1$, and the accumulated dispersion from the beginning of the system to the beginning of the fiber is now $D_a^{(k)} \triangleq \sum_{i=1}^{k-1} D_i l_i$.

Reasoning as before, the XPM contribution

$$d\theta_{sp}^{(k)}(z,\omega) = -2\gamma_k P_p(L_k+z,\omega)dz \tag{18}$$

generated at coordinate z of the k-th fiber enters a "purely linear equivalent fiber" so that its contribution to the relative output amplitude distortion on the probe is

$$\frac{dA_{sp}^{(k)}(z,\omega)}{<A_s>} = -\sin\left[\omega^2\frac{\lambda^2}{4\pi c}(D_r^{(k)}-D_kz)\right]d\theta_{sp}^{(k)}(z,\omega) \tag{19}$$

The residual accumulated dispersion from the beginning of the k-th link to the end of the system is now $D_r^{(k)} \triangleq \sum_{i=k}^{M} D_i l_i$. Integrating as before over the k-th fiber length and adding the contributions of all fiber segments, the overall XPM/AM filter for the M links becomes: $H_{sp}(\omega) = \sum_{k=1}^{M} C_p^{(k)} H_{sp}^{(k)}(\omega)$, where $H_{sp}^{(k)}(\omega)$ is given by (16) with the appropriate parameters of the k-th fiber. The relative probe power distortion at the system end is given again by eq. (15).

When several pump channels are present, the total relative probe amplitude distortion can be written as the sum of the contributions due to each pump:

$$\frac{\Delta A_s(\omega)}{<A_s>} = \sum_{p \neq s} P_p(0,\omega) H_{sp}(\omega) \tag{20}$$

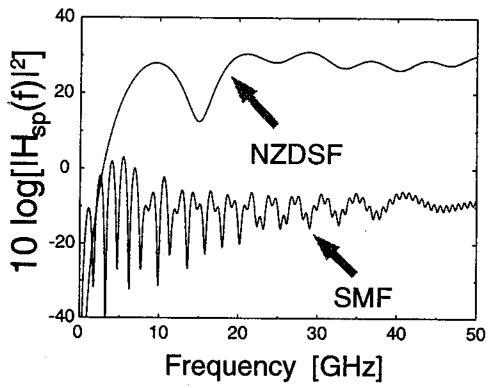

Fig. 3. Square magnitude of the XPM filter for a single span 50 km long.

In Fig. 3 the square magnitude of the filter (16), multiplied by two to give the power distortion (under the further approximation seen in section 2), is plotted for a single span 50 km long, fully compensated by an ideal linear fiber, for two different transmission fiber: a SMF, with dispersion 17 ps/km/nm, and a non-zero dispersion-shifted fiber (NZDSF), with dispersion ± 2 ps/km/nm. It is evident that the filtering action is more effective for the SMF, being the curve lower. This is due to the well-known filtering effect of walk-off [12].

3.1 Simulation Results

In Fig. 4 and Fig. 5 we compare the results of computer simulations performed with a split-step Fourier method [4], with the predictions of eq. (15). Simulations include the effects of GVD, SPM and XPM for the pump, and GVD and XPM (no SPM) for the probe, to highlight the precision of formula (15). Simulations are carried out for a 5 span WDM system, perfectly compensated after each span, with 5 dBm peak power for both pump and probe, and channel spacing $\Delta\lambda = 0.8$ nm. The probe is CW, while the pump is on-off keying (OOK) modulated with nonreturn-to-zero (NRZ) raised cosine pulses (roll-off 0.8) at a bit rate $R = 10$ Gb/s for Fig. 4, and 40 Gb/s for Fig. 5.

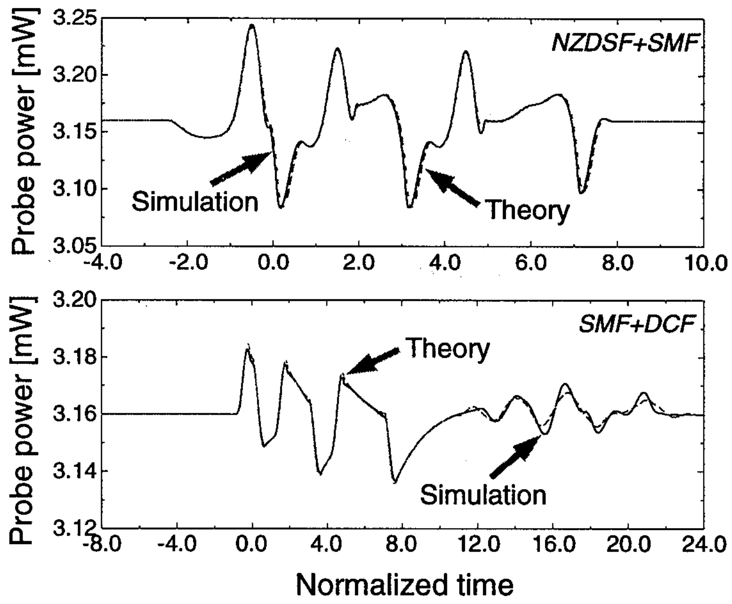

Fig. 4. Simulations of two 10 Gb/s systems, $M = 5$ spans, $\Delta\lambda = 0.8$ nm. Top row: NZDSF+SMF system. Bottom row: SMF+DCF system. Time is normalized to the bit time 1/R.

Fiber	Dispersion $[ps/km/nm]$	Slope $[ps/km/nm^2]$	Effective area $[\mu m^2]$	Nonlinear coefficient $10^{-20}[m^2/W]$	Attenuation $[dB/km]$
SMF	17	0.07	80	2.7	0.22
NZDSF	-2	0.07	57	2.7	0.22
DCF	-100	0.09	20	2.6	0.6

Table 1. Fiber parameters.

Top graphs refer to a system in which the transmission fiber for each span is a negative NZDSF, with length $l = 100$ km, and a SMF, with length $l = 11.765$ km, is used for span compensation. Bottom graphs refers to a system in which the transmission fiber is a SMF, with $l = 100$ km, and a dispersion compensating fiber (DCF), with $l = 21.25$ km, is used for compensation. Fiber parameters are given in Table 1.

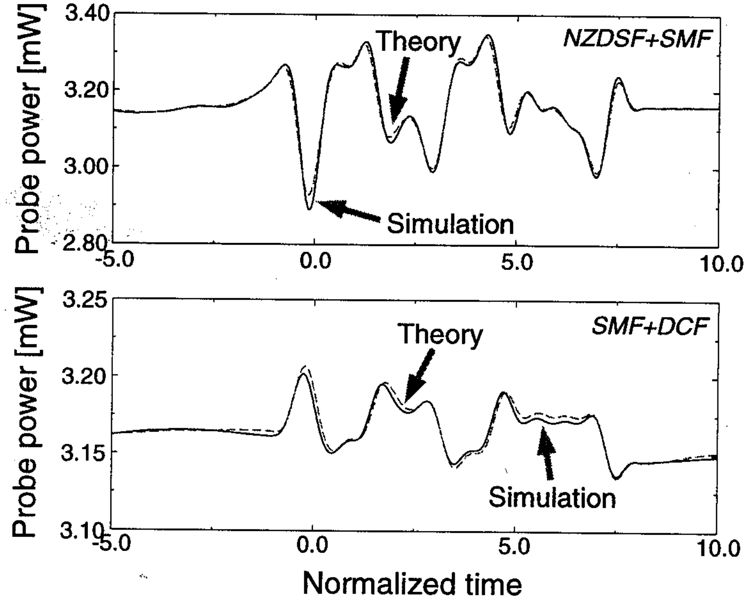

Fig. 5. Simulations of two 40 Gb/s systems, $M = 5$ spans, $\Delta\lambda = 0.8$ nm. Top row: NZDSF+SMF system. Bottom row: SMF+DCF system. Time is normalized to the bit time 1/R.

In both systems, the wavelength of exact compensation is halfway between channels. The figures show the probe output power, both simulated and predicted by eq. (15). As seen from Fig. 4, the accuracy of the improved model is the same as of the one presented in [9] at the bit rate of 10 Gb/s. On the other hand such model failed at the bit rate of 40 Gb/s, while the improved one is still valid (Fig. 5).

As already mentioned, SPM was intentionally not included in the simulation of the probe, in order to check the accuracy of the theory, which only accounts for XPM. In Fig. 6 we show simulated results in which the SPM on the probe is either OFF (dashed line) or ON (solid line). As we can see, the SPM caused by the XPM-induced intensity noise (XPM/IN) tends to increase the intensity fluctuations. Hence our model tends to underestimate the variance of the overall kerr-induced intensity noise on the probe channel. The difference between dashed and solid curves in the SMF+DCF system is somehow surprising, since the SPM caused by the XPM-induced intensity noise should be a second-order effect, and hence one would guess it to be much smaller than the XPM/IN causing it. The reason why it is indeed larger than the XPM/IN is the following: the XPM/IN is mostly reabsorbed by compensation, as the XPM is mostly generated at the beginning of the link, where power is large. SPM induced by XPM/IN is most efficienly generated away from the input, although not too much, since the power must still be large enough. Thus the

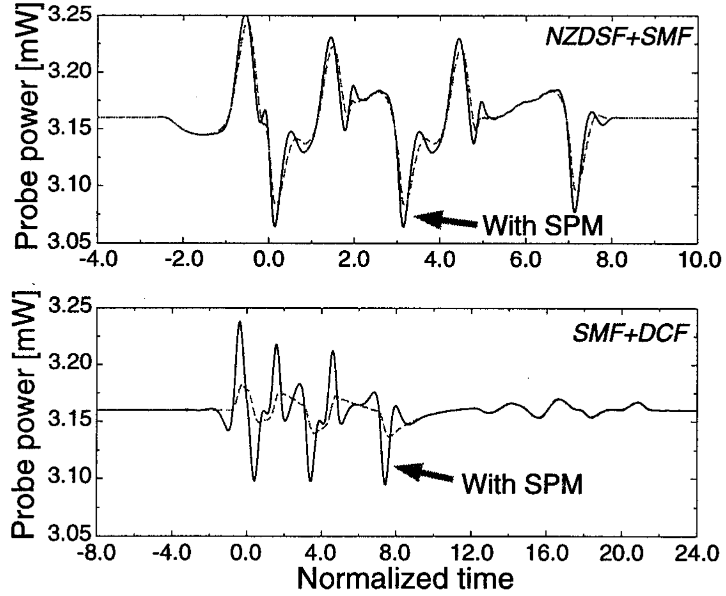

Fig. 6. Simulations of two 10 Gb/s systems, $M = 5$ spans, $\Delta\lambda = 0.8$ nm, with and without SPM. Top row: NZDSF+SMF system. Bottom row: SMF+DCF system. Time is normalized to the bit time 1/R.

IM induced by such SPM cannot be completely reabsorbed by compensation. This is particularly true for large-dispersion fibers, as we can see from the bottom figure. In the same figure, we can also note that, in the region on the left, the XPM/IN is generated in the transmission fiber and, therefore, is almost completely reabsorbed during compensation, making the SPM induced by it prevalent on the residual XPM/IN. In the region on the right, in which the XPM is generated in the compensating fiber by the same bits (shifted because of walk-off [12]), the XPM/IN is not reabsorbed during compensation, and the induced SPM is not negligible. This means that the effect of the induced SPM is not negligible when the XPM/IN which induced it is minimized by compensation. On the other hand, a non-optimal compensation is sufficient to make negligible the relative weight of such effect.

4. Intensity Distortion Induced by SPM

In this Section, we will apply the same method as in Section 3 to cope with the intensity distortion induced by SPM.

Consider one span of single-mode fiber of length L, with a linearly-polarized intensity modulated input signal, having zero initial phase. Let the Fourier transform of the input intensity $P_{in}(t) = a_{in}(t)^2$ be $P(0,\omega)$. Let's find the SPM generated at coordinate $0 < z < L$ along the fiber. Assuming that the signal up to coordinate z *is distorted by GVD only*, according to the Wang–Petermann model ([1], eq. (27)), its intensity has Fourier transform (referred to a time frame moving with the signal group velocity) given by: $P(z,\omega) = P(0,\omega)e^{-\alpha z}\cos\left(\omega^2 \frac{\lambda^2}{4\pi c} Dz\right)$ where the cosine term accounts for the IM/IM conversion caused by the intensity perturbation $P(0,\omega)$ in ([1], eq. (27)), and we took into account the fiber attenuation per unity length α since the power level at z matters in determining SPM. The phase induced at z through SPM by propagation of the signal over an infinitesimal segment dz is [11]: $d\theta_{spm}(z,\omega) = -\gamma P(z,\omega)\,dz$, where γ is the nonlinear Kerr coefficient. Such phase modulation enters the remaining $L-z$ km of fiber: if such fiber were affected by GVD only, it would produce an infinitesimal relative magnitude distortion at its output, obtained using (10) as:

$$\frac{dA_{spm}(z,\omega)}{<A>} = -\sin\left(\omega^2 \frac{\lambda^2}{4\pi c} D(L-z)\right) d\theta_{spm}(z,\omega) \tag{21}$$

where $<A>$ is the average output field magnitude. The SPM induced by such infinitesimal magnitude distortion is neglected.

The total output relative magnitude distortion induced by SPM is obtained integrating (21) in dz over the fiber length:

$$\frac{\Delta A_{spm}(\omega)}{<A>} = P(0,\omega) H^{AM}_{spm}(\omega) \tag{22}$$

where we defined the SPM/AM conversion filter as:

$$H^{AM}_{spm}(\omega) \triangleq \gamma \int_0^L \left\{ e^{-\alpha z}\cos\left(\omega^2 \frac{\lambda^2}{4\pi c} Dz\right) \sin\left(\omega^2 \frac{\lambda^2}{4\pi c} D(L-z)\right)\right\} dz \tag{23}$$

Such integral can be computed as:

$$\begin{aligned} H^{AM}_{spm}(\omega) = \gamma \Bigg\{ & \frac{1}{4j} e^{j\omega^2 \frac{\lambda^2}{4\pi c}(D_r - D_a)} \frac{1 - e^{\left(-\alpha - 2jD\omega^2 \frac{\lambda^2}{4\pi c}\right)L}}{\alpha + 2jD\omega^2 \frac{\lambda^2}{4\pi c}} \\ & - \frac{1}{4j} e^{-j\omega^2 \frac{\lambda^2}{4\pi c}(D_r - D_a)} \frac{1 - e^{\left(-\alpha + 2jD\omega^2 \frac{\lambda^2}{4\pi c}\right)L}}{\alpha - 2jD\omega^2 \frac{\lambda^2}{4\pi c}} \\ & + \frac{1}{2}\sin\left[\frac{\lambda^2}{4\pi c}\omega^2 (D_r + D_a)\right] \frac{1 - e^{-\alpha L}}{\alpha} \Bigg\} \end{aligned} \tag{24}$$

where D_r is the residual dispersion accumulated from the beginning of the fiber to the end of the system, here $D_r = DL$, and D_a is the dispersion accumulated from the beginning of the system to the beginning of the fiber, here $D_a = 0$.

Consider now the general case of a chain of M end-amplified fiber links, with $\alpha_i, \gamma_i, D_i, l_i$, the attenuation, nonlinear and dispersion coefficients, and the length of the i-th link, $i = 1, \ldots, M$, respectively. Suppose that the i-th amplifier has gain $G_s^{(i)}$ for the signal, so that the signal intensity at coordinate z of the k-th link, in our assumptions, is

$$P(L_k + z, \omega) = C_s^{(k)} P(0,\omega) e^{(-\alpha_k)z} \cos\left[\omega^2 \frac{\lambda^2}{4\pi c}(D_a^{(k)} + D_k z)\right]$$

where $L_k \triangleq \sum_{i=1}^{k-1} l_i$, $C_s^{(k)} \triangleq \prod_{i=1}^{k-1} e^{(-\alpha_i) l_i} G_s^{(i)}$, $C_s^{(1)} \triangleq 1$, and the accumulated dispersion from the beginning of the system to the beginning of the fiber is now $D_a^{(k)} \triangleq \sum_{i=1}^{k-1} D_i l_i$. Reasoning as before, the SPM contribution $d\theta^{(k)}_{spm}(z,\omega) = -\gamma_k P(L_k + z, \omega) dz$ generated at coordinate z of the k-th fiber enters a "purely linear equivalent fiber" so that its contribution to the relative output magnitude distortion is

$$\frac{dA^{(k)}_{spm}(z,\omega)}{<A>} = -\sin\left[\omega^2 \frac{\lambda^2}{4\pi c}(D_r^{(k)} - D_k z)\right] d\theta^{(k)}_{spm}(z,\omega)$$

The residual accumulated dispersion from the beginning of the k-th link to the end of the system is now $D_r^{(k)} \triangleq \sum_{i=k}^{M} D_i l_i$. Integrating as before over the k-th fiber length and adding the contributions of all fiber segments, the overall SPM/AM conversion filter for the M-link system becomes: $H^{AM}_{spm}(\omega) = \sum_{k=1}^{M} C_s^{(k)} H^{(k)}_{spm}(\omega)$, where $H^{(k)}_{spm}(\omega)$ is given by (24) with the appropriate parameters of the k-th fiber. The signal relative magnitude distortion at the system end is given again by eq. (22).

Although such results could be put in terms of the output signal relative *intensity* distortion by using ([1], eq. (27)) instead of (10), it is found that the field approach is more accurate than the intensity approach, as already verified in Section 2.

Finally, if the effects of GVD and SPM add up, the output field magnitude is obtained from (9) and (22), as:

$$a_{out}(t) \simeq <A> \left(h^{AM}_{spm}(t) \otimes a^2_{in}(t) - h_I(t) \otimes \theta_{in}(t)\right) + h_R(t) \otimes a_{in}(t) \tag{25}$$

where $h^{AM}_{spm}(t)$ is the inverse transform of (24), and $h_R(t)$ and $h_I(t)$ indicate the real and imaginary impulse responses of the concatenation of fibers composing the (possibly compensated) system.

An important comment must be made on eq. (25). Such equation was derived under the hypothesis of small perturbations around the average value of the signal amplitude $<A>$. In the case of SPM such hypothesis is clearly violated, being the intensity variations at the input due to the on-off modulation of the signal itself. On the other hand, we can think that these variations are relative, rather than to the average value, to the instantaneous signal value, for which we have an approximate expression if GVD only contributes to its distortion. In this case, $<A>$ is replaced, in eq. (25), by $h_R(t) \otimes a_{in}(t)$, (indeed by its absolute value, being the intensity a positive quantity). Even if not readily analytically justifiable, this empirical choice allows to obtain much better results than these obtained using <A>. Therefore in the results we used the formula:

$$a_{out}(t) \simeq |h_R(t) \otimes a_{in}(t)| \left[h_{spm}^{AM}(t) \otimes a_{in}^2(t) - h_I(t) \otimes \theta_{in}(t) + 1\right] \qquad (26)$$

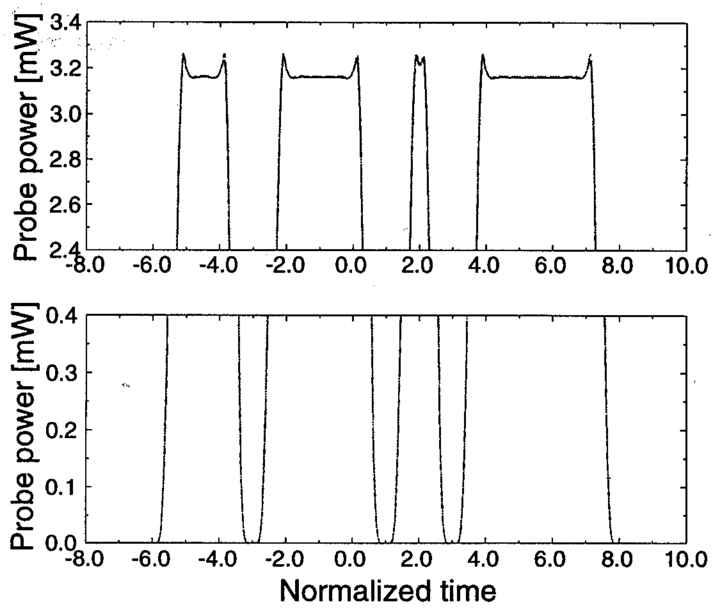

Fig. 7. Simulations of a 10 Gb/s NZDSF+SMF system, $M = 5$ spans. Top row: details of crests (marks). Bottom row: details of troughs (spaces). Time is normalized to the bit time 1/R.

4.1 Simulation Results

In Fig. 7 and Fig. 8 we compare the predictions of eq. (26) with the results of computer simulations, performed once again for the two systems composed of 5 spans of NZDSF and SMF, respectively, and perfectly compensated at each span. Only one channel at 10 Gb/s is propagated, with the peak power of 5 dBm. Figures show the output intensity, with details of the space (top) and mark (bottom) bits. The accuracy of the prediction is quite good for the first system, while for the one based on SMF (because of the higher dispersion) the effects of SPM are a little underestimated. Other simulations have shown that the error grows proportionally with the number of spans. This means that the model cannot be used if an accurate estimate of SPM is required. On the other hand, the model well captures the mechanism of the interaction between GVD and SPM, and can therefore be used for a theoretical study of such mechanism.

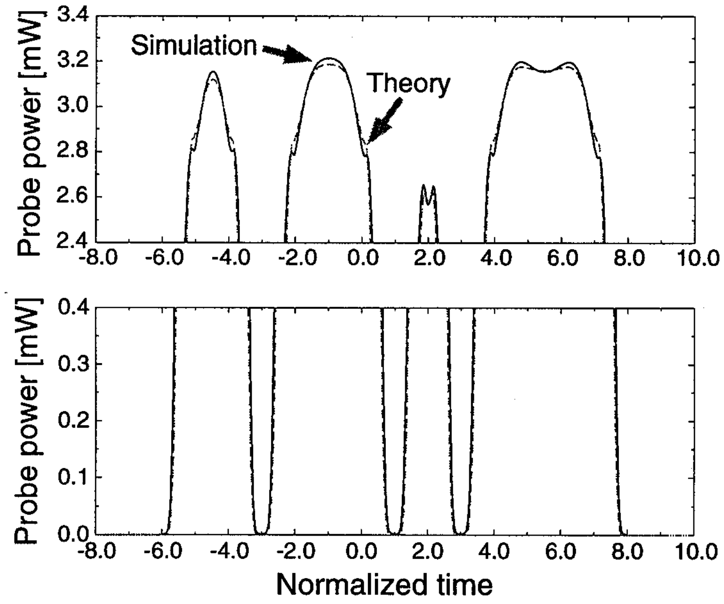

Fig. 8. Simulations of a 10 Gb/s SMF+DCF system, $M = 5$ spans. Top row: details of crests (marks). Bottom row: details of troughs (spaces). Time is normalized to the bit time 1/R.

5. Conclusion

In this paper we introduced a new linear model for the intensity distortion induced by XPM and SPM in dispersion compensated transmission systems. By comparison to simulations we have shown that the model well captures the essence of the interaction between nonlinear phase modulation and GVD, giving quite accurate predictions of the signal distortion, especially in the case of XPM, within a large applicability range.

References

[1] J. Wang and K. Petermann, "Small signal analysis for dispersive optical fiber communication system," *IEEE J. Lightwave Technol.*, vol. 10, pp. 96-100, Jan. 1992.

[2] S. Bigo, D. Penninckx, and M. W. Chbat, "Investigation of self-phase modulation limitation on 10-Gbit/s transmission over different types of fiber," *Proc. OFC'98*, pp. 389-390, Feb. 1998.

[3] S. Bigo, G. Bellotti, and M. W. Chbat, "Investigation of cross-phase modulation limitation over various types of fiber infrastructures," *IEEE Photon. Technol. Lett.*, vol. 11, pp. 605-607, May 1999.

[4] G. P. Agrawal, *Nonlinear Fiber Optics*, 2nd ed. New York: Academic, 1995.

[5] N. Kikuchi and S. Sasaki, "Analytical evaluation of self-phase modulation effect on the performance of cascaded optical amplifier systems," *IEEE J. Lightwave Technol.*, vol. 13, pp. 868-878, May. 1995.
[6] R. Hui, Y. Wang, K. Demarest, and C. Allen, "Frequency response of cross-phase modulation in multispan WDM optical fiber systems," *IEEE Photon. Technol. Lett.*, vol. 10, pp. 1271-1273, Sep. 1998.
[7] A. V. T. Cartaxo, "Impact of modulation frequency on cross-phase modulation effect in intensity modulation-direct detection WDM systems," *IEEE Photon. Technol. Lett.*, vol. 10, pp. 1268-1270, Sep. 1998.
[8] G. Bellotti, M. Varani, C. Francia, and A. Bononi, "Intensity/cross-phase/intensity conversion filters in dispersion compensated multiwavelength transmission systems," *1998 Conference on Information Science and Systems*, Princeton, NJ, paper TP4.2, Mar. 1998.
[9] G. Bellotti, M. Varani, C. Francia, and A. Bononi, "Intensity distortion induced by cross-phase modulation and chromatic dispersion in optical-fiber transmissions with dispersion compensation," *IEEE Photon. Technol. Lett.*, vol. 10, pp. 1745-1747, Dec. 1998.
[10] M. Shtaif and M. Eiselt, "Analysis of intensity interference caused by cross-phase modulation in dispersive optical fibers," *IEEE Photon. Technol. Lett.*, vol. 10, pp. 979-981, July 1998.
[11] D. Marcuse, *Theory of Dielectic Optical Waveguides*, 2nd ed. Kriegel, 1989.
[12] A. Bononi, C. Francia, and G. Bellotti, "Impulse response of cross-phase modulation filters in multi-span transmission systems with dispersion compensation," *Optical Fiber Technology*, vol. 4, pp. 371-383, Dec. 1998.

Authors' Index